

Brazilian Journal of Radiation Sciences ISSN: 2319-0612 Sociedade Brasileira de Proteção Radiológica

Fungaro, D. A.; Grosche, L. C.; Silva, P. C. S.
Physicochemical and radiological characterization offlue gas
desulfuration waste samples from Brazilian coal-fired power plants
Brazilian Journal of Radiation Sciences, vol. 11, no. 2, e2275, 2023, April-June
Sociedade Brasileira de Proteção Radiológica

DOI: https://doi.org/10.15392/2319-0612.2023.2275

Available in: https://www.redalyc.org/articulo.oa?id=722277919011



Complete issue

More information about this article

Journal's webpage in redalyc.org



Scientific Information System Redalyc

Network of Scientific Journals from Latin America and the Caribbean, Spain and Portugal

Project academic non-profit, developed under the open access initiative



OF RADIATION SCIENCES 11-02 (2023) | 01-18 | e2275





Physicochemical and radiological characterization of flue gas desulfuration waste samples from Brazilian coal-fired power plants

Fungaro^a, D.A.; Grosche^a, L.C.; Silva^a, P.C.S.

^a Instituto de Pesquisas Energéticas e Nucleares (IPEN / CNEN - SP) Av. Professor Lineu Prestes 2242
05508-000 São Paulo, SP, Brazil
dfungaro@ipen.br

ABSTRACT

Flue gas desulfurization (FGD) waste is an industrial by-product generated during the flue gas desulfurization process in coal-fired power plants. This by-product contain trace quantities of naturally occurring radionuclides and elements such as As, Ba, Co, Cr, Zn. The characteristics of FGD waste are important for its reuse and are mainly depend on the desulfurization process. In this work, two types of FGD materials collected from three coal-fired power plants using semi-dry and wet processes were characterized by X-Ray Diffraction (XRD), Scanning Electron Microscope (SEM), X-ray fluorescence (XFR) and particle size analysis. The radioactive content of ²³⁸U, ²³²Th, ²²⁸Th, ²²⁶Ra, ²²⁸Ra, ²¹⁰Pb and ⁴⁰K and trace elements were also determined using Neutron activation analysis and Gamma-ray spectrometry. The major constituents for all samples were Ca, Si, S, Al and Fe. Wet FGD by-product presented also high magnesium content. The wastes contain mainly semi-hydrate calcium sulfite and calcium sulfate. The particle size of FGD from semi-dry process was lower than that from the wet process. The average activity concentration of ²³⁸U, ²³²Th, ²²⁶Ra, ²¹⁰Pb, ²²⁸Ra, ²²⁸Th and ⁴⁰K varied between were 50-71, 33-42, 28-52, 113-150, 26-33, 33-39, 161-390 Bq kg⁻¹, respectively. According to the results of leaching and solubilization tests, FGD samples were classified as non-hazardous and non-inert. The obtained data are useful for evaluation of possible applications of FGD by-products.

Keywords: Coal combustion, FGD waste, Characterization.

ISSN: 2319-0612

DOI: https://doi.org/10.15392/2319-0612.2023.2275

Submitted: 2023-03-22 Accepted: 2023-06-13



1. INTRODUCTION

Coal-fired power plants are a major source of emissions of air pollutants including SO₂, NOx, particulate matter, among others. The sulfur dioxide (SO₂) combines with water and air forming sulfuric acid, which is the main component of acid rain.

Flue gas desulfurization (FGD) is the most used technology for reducing sulfur oxide emissions and remove up to 99% of the sulfur oxides in flue gas for a typical conventional coal-fired power plant [1].

FGD systems are generally classified as wet, semi-dry or dry processes. The wet FGD process is based on an acid-base reaction that takes place under oxidation conditions. Sulfur oxides in flue gas react with CaCO₃ and MgCO₃ to produce 90% gypsum (CaSO₄.2H₂O) and hannebachite (CaSO₃.½H₂O) in forced oxidation. FGD by-product of wet process is also also known as FGD gypsum [1-3].

In dry and semi-dry FGD processes, the sulfur oxide in the flue gas reacts with $Ca(OH)_2$ (or CaO) and an excess of water to produce a slurry. This slurry is nebulized in a spray dry absorber, where SO_2 is removed from the flue gas. The resulting by-product of this process is a dry mixture of hannebachite ($CaSO_3 \cdot \frac{1}{2}H_2O$) with minor amounts of gypsum [1].

Large volumes of FGD wastes from wet, dry or semi-dry FGD process are expected to be continuously produced with the increasing activity of coal-fired power plants.

FGD waste is discarded in landfills on the surrounding of the coal-fired thermal plant. For FGD gypsum, exists a market demand as a substitute of natural gypsum. However, dry or semi-dry FGD by-products are currently not widely used due to its high content of calcium sulfite. There have been some reports on the use as cement additives and in the manufacture of sulfoaluminate cement [4].

Presently, continuous research is ongoing on the use of FGD wastes for more advanced applications, such as zeolite synthesis [5, 6].

FGD waste belong to complex composite materials with variable physical properties, particle morphology and chemical composition. FGD waste contain also trace quantities of naturally occurring radionuclides from the uranium and thorium series, as well as other naturally occurring radionuclides such as ⁴⁰K derived from the original coal matrix that tend to become enriched in their by-products. Thus, it is important to analyze their properties in order to address the potential reuse of FDG wastes [7-9].

The aim of this investigation is to compare the physicochemical characteristics of FGDs byproducts produced using wet and semi-dry process from three Brazilian thermal power plant. In addition, radiation characterization was performed to assess the possible radiological risks to human health due to the use of such materials.

2. MATERIALS AND METHODS

2.1. Material

All chemicals that are used in this study were of analytical grade. Three types of samples of different origin were studied here. The waste produced from the wet flue gas desulfurization process was collected at President Medici coal-fired power plant, located in Candiota, Rio Grande do Sul, Brazil (FGD-C). The semi-dry samples were collected at Pecem coal-fired power plant (FGD-P) located in São Gonçalo do Amarante, Ceará, Brazil and Itaqui coal-fired power plant (FGD-I) located in São Luís, Maranhão, Brazil.

2.2. Characterization of materials

Samples were characterized in terms of semi-quantitative chemical composition by X-ray fluorescence (Rigaku – RIX 3000). A scanning electron microscope was used to verify the morphology of the samples (Philips XL 30). The mineralogical composition was determined by X-ray diffraction (Rigaku – Multiflex) using Cu Kα radiation at 40 kV and 20 mA. The particle size distribution for the samples was determined using a laser diffraction particle size analyzer (Malvern – Mastersizer 2000). Leaching and solublization experiments were performed following the Brazilian Association of Technical Standards Norm [10, 11]. The concentration of elements was determined in the resulting leachate and solubilized extracts by inductively coupled plasma optical emission spectrometry using a Spectro ARCOS ICP OES (Kleve, NRW, Germany).

Neutron activation analysis was used to determine the concentrations of the elements U and Th. For this determination, approximately 100 mg of the sample were weighted and packed in polyethylene bags and irradiated in the IEA-R1 nuclear research reactor, at IPEN, in a neutron flux of 10^{12} n cm⁻² s⁻¹ for a period of 8 hours. Reference materials USGS STM-2, NIST SRM 1646a and a paper filter pipetted with a standard solution of the interest elements were also prepared and irradiated together with the samples to calculate the concentrations by the comparative method. After

the irradiation, two sets of measurement were done. The first, after a one week period of cooling, to determine U concentrations and, the second, after two weeks, to determine Th concentration. Samples were counted for a period of 5000 s, in the first and second measurement, by using an EG&G Ortec Ge high pure Gamma Spectrometer detector (AMETEK Inc., USA) and associated electronics, with a resolution of 0.88 and 1.90 keV for 57Co (122 keV) and 60Co (1332 keV), respectively [12]. Activity concentrations of U and Th were obtained by their specific activity using the conversion factor of 24.5 and 4.05, respectively.

Instrumental neutron activation analysis was also applied to determine trace elements. For this multi-elemental analysis, approximately 150 mg of samples and reference materials (NIST 1646a Estuarine Sediment and USGS STM-2 Table Mountain Syenite, and synthetic standards prepared by pipetting appropriate aliquots of standard solutions (SPEX CERTIPREP) onto small sheets of Whatman No. 41 filter paper) were accurately weighed and sealed in pre-cleaned double polyethylene bags for irradiation. Samples and reference materials were irradiated for 8 h in a thermal neutron flux of 10^{12} cm⁻² s⁻¹ in the IEA-R1 nuclear research reactor at IPEN (Instituto de Pesquisas Energéticas e Nucleares, Brazil). Counting was done at different time frames, depending on the radionuclide halflife produced during the irradiation. Gamma Spectrometry was performed by using an EG&G Ortec Ge Highpure Gamma Spectrometer detector (AMETEK Inc., USA) and associated electronics, with a resolution of 0.88 and 1.90 keV for ⁵⁷Co and ⁶⁰Co, respectively. The analysis of the data was done by using an in-house gamma ray software, VISPECT program, to identify the gamma each energy transition. Methodology validation was performed by analyzing the same reference materials cited above. The results presented are mean values (mg kg⁻¹) for the duplicate and standard deviation for concentrations of elements. The relative standard deviations and relative errors were lower than 10% for most of the elements determined.

The concentration of the natural radionuclides ²²⁶Ra, ²²⁸Ra, ²¹⁰Pb and ⁴⁰K were carried out by non-destructive γ-ray spectrometry. Samples were packed in 50 cm³ polypropylene cylindrical containers and they were kept sealed for at least 30 days in order to reach radioactive equilibrium between ²²⁶Ra and ²²²Rn progenies. A HPGe EG&G Ortec detector with 40% of relative efficiency and 2.09 keV resolution at 1.33 MeV and associated electronic devices were used, with live counting time of 80,000 s. The spectra were acquired by multichannel analyzer and, for the analysis, Genie 2000 software package was used. The activity concentration for ²¹⁰Pb in the samples was corrected

for self-absorption according to the method described in [13]. The detector efficiency was calibrated by using the reference material IAEA-RGU-1, IAEA-RGTh-1 and IAEA-RGK-1.

3. RESULTS AND DISCUSSION

3.1. Radiological Properties

The activity concentrations of naturally occurring radionuclides in different FGD samples is shown in Table 1. The data give an idea of the variability found in FGD samples coming from different sources. FDGD-I and FDG-P were generated in plants that use coal mainly from Colombia, while FGD-C is generated in a plant that uses coal from southern Brazil. In general, the activity concentrations of ⁴⁰K is higher in FGD samples of semi-dry process (FGD-P. FGD-I) than in FGD sample of wet process gypsum (FGD-C). Also, ²¹⁰Pb, ²³⁸U and ²³²Th showed the highest activity in FGD-P.

Table 1: Activity concentration in FGD samples from the three thermal power stations

Sample	Activity concentration(Bq kg ⁻¹)*						
	²³⁸ U	²³² Th	²²⁶ Ra	²¹⁰ Pb	²²⁸ Ra	²²⁸ Th	40 K
FGD-C	50 ± 6	38 ±2	28±3	117±22	26±1	36±2	161±9
FGD-I	54 ± 3	33±2	52±2	113±20	28±1	33±2	283±14
FGD-P	71 ± 9	42±1	52±2	150±26	33±1	39±2	390±18

^(*) mean \pm s.d.

Comparing the present results, the activity concentrations in FGD samples were lower than the worldwide average values of 200, 200, 200 Bq kg⁻¹ for 238 U, 226 Ra, 232 Th respectively, and 500 Bq kg⁻¹ for 40 K for fly ash [14].

There are few studies in the literature on the radionuclide activity concentrations in FGD samples. Roper (2012) determined the activity concentrations of 20 samples of FGD gypsum and the following results were found (mean and range values): 9 (1-24) for 238 U, 1 (0.2-3) for 232 Th, and 10 (2-19) for 40 K. Kardos et al., reported that the results of activity concentration of FGD gypsum with standard deviation were 13 ± 3 for 40 K and 22 ± 3 for 226 Ra [15].

3.2. Physicochemical Properties

3.2.1. Concentration of trace elements in FGD samples

During the coal combustion process, trace elements (e.g., As, Se and Hg) are decomposed by heat and travel with the flue gas. These trace elements may be captured during the desulfurization process and become part of FGD by-product. In addition, trace elements are captured by fly ash.

The elements of greater concern are As, Cd, Hg, Pb, Se and Zn, due to their potentially detrimental impact on human health and the environment.

Table 2 shows the concentrations of trace elements in FGD samples determined by neutron activation. The elements that showed the highest concentrations in decreasing order were Ba> Rb> Zr > Ce. The concentration of As, Ce, Co, Cr, Cs Eu, Hf, La, Lu, Nd, Sm, Ta, Tb, Yb in the three FGD samples were similar.

The main source of most of these elements is limestone because it is associated with the highly insoluble Al-Si fraction of this reagent. The elements Hf, Ta, Ce, Eu, Tb, Yb and Zn are mainly retained in the particulate form and selenium is captured by the FGD in a gaseous form and/or as particulate matter [1, 16, 17].

The concentration of some trace elements found in the semi-dry FGD samples (FGD-I and FGD-P) is higher than in the wet FGD sample (FGD-C). During the oxidation of the wet FGD material, many of the trace elements are partitioned to the liquid phase because of recrystallization purification as well as pH adjustment to the 4.5 necessary for air oxidation [18].

FGD materials can vary widely in their properties depending on their source. However, the concentration of Co, Cr, Se and Zn for the dry FGD samples is within the concentration range found in 59 samples collected from 13 locations representing four major FGD scrubbing technologies of U.S.A [19]. Also, As, Ba, Br, Co, Cr, Rb, Se and Zn concentrations are within the values reported in the reviewed literature [20].

In general, trace element concentrations were higher in the fly ash than in the FGD gypsum (FGD-C) collected from the same power plant [21].

Table 2: Concentration of trace elements in FGD samples (mg Kg⁻¹)

	FGD-C	FGD-I	FGD-P	
As	24.4±0.3	25±2	33.7±0.4	
Ba	120±12	723±45	1009±39	
Br	2.75 ± 0.09	8.3 ± 0.2	7.6 ± 0.2	
Ce	48±2	42±2	53±1	
Co	24.4 ± 0.4	25.3±0.4	33.7±0.3	
Cr	24.4 ± 0.8	25.3±0.7	33.7±0.8	
Cs	24 ± 2	25±1	34 ± 2	
Eu	0.66 ± 0.02	1.04 ± 0.03	1.01 ± 0.02	
Hf	3.38 ± 0.05	4.13±0.06	4.41 ± 0.04	
La	23.9 ± 0.5	17.6±0.3	28.1±0.6	
Lu	0.31 ± 0.01	0.34 ± 0.02	0.38 ± 0.01	
Nd	24±1	19±1	33±1	
Rb	59±3	60±3	82±3	
Sb	0.85 ± 0.02	5.4 ± 0.2	5.68 ± 0.04	
Sc	7.18 ± 0.04	12.48 ± 0.05	18.30±0.06	
Se	1.80 ± 0.22	11.18±0.61	18.05 ± 0.21	
Sm	4.1 ± 0.1	4.1 ± 0.1	4.7 ± 0.1	
Ta	0.45 ± 0.01	0.50 ± 0.04	0.27 ± 0.07	
Tb	0.58 ± 0.06	0.52 ± 0.06	0.49 ± 0.09	
Yb	3.1 ± 0.4	2.1 ± 0.1	3.1 ± 0.4	
Zn	49±2	114 ±4	119±3	
Zr	-	169±73	246±32	

3.2.2 Chemical composition

The chemical composition of FGD wastes and loss on ignition (LOI) obtained by X-ray fluorescence is given in Table 3. As can be seen from Table 3, the major constituents were Ca, Si, S, Al and Fe. The high magnesium content in FGD-C sample is justified because in the wet process Mg²⁺ such as slaked lime (Ca(OH)₂) or magnesium-containing slaked lime (Ca(OH)₂ and Mg(OH)₂) is used to improve the oxidation efficiency of coal combustion products, thus increasing the amount of gypsum produced. The percentage of elements is within the range usually encountered in flue gas desulfurization (FGD) by-product [20].

Table 3: Chemical composition (wt%) of FGD samples

FGD-C FGD-P FGD-I

CaO	26.3	22.1	22.8
SiO_2	22.2	31.4	30.8
MgO	13.4	1.5	1.61
SO_3	11.2	11.9	10.7
Al_2O_3	6.76	12.4	13.5
Fe_2O_3	2.39	6.22	5.71
K_2O	0.873	1.6	1.48
TiO_2	0.328	0.772	0.65
MnO	0.026	0.043	0.06
CoO	0.024	< 0.001	-
WO_3	0.023	< 0.001	-
SrO_2	0.022	0.063	0.02
V_2O_5	0.014	< 0.001	0.06
ZrO	0.014	0.018	0.01
ZnO	0.009	0.022	0.02
Na ₂ O	< 0.001	0.937	0.56
P_2O_5	< 0.001	0,134	0.11
Cl	< 0.001	0.16	0.13
Cr_2O_3	< 0.001	0.018	0.01
NiO	< 0,.001	0.011	0.01
BaO	< 0.001	0.12	-
Rb_2O	-	-	0.01
CuO	-	-	0.01
PbO	-	-	0.01
LOI	16.3	10.6	11.8

An important parameter relating to the unburned carbon content is LOI (loss of ignition). As can be seen from Table 3, the highest value of LOI has FGD-C. The large percentage of loss of ignition may be an advantage over some applications that require a high coal content.

3.2.3. Particle size distribution

Figure 1 shows the differential and cumulative particle size distributions for FGD samples. The particle size distributions of material are given in Table 4. The differential size distribution of the material is relatively uniform with the expected normal bell-shaped distribution curve for FGD-C and FGD-I samples. The FDG-P sample showed a bimodal particle distribution curve.

These distributions specify that the majority of particles (90%) lie below 90 μ m for semi-dry process (FGD-P and FGD-I) and below 194 μ m for wet process (FGD-C). The particle size distribution for FGD-C samples is broader than for FGD-P and FGD-I.

Particle size is affected by the FGD process, and the ash size from the semi-dry process is lower than that from the wet process. In wet process, forced oxidation, which is a separate step after the actual desulfurization process, involves blowing air into the tank that holds calcium sulfite sludge, and results in the oxidation of the calcium sulfite (CaSO₃) to calcium sulfate (CaSO₄). The calcium sulfate formed by this reaction grows to a larger crystal size than calcium sulfite. It was reported that gypsum from full-scale plants present $d_{50} = 34.9 - 41.3 \mu m$ [22].

100 a 3.5 80 2.5 40 1.5 20 Particle Size (µm) 100 b 80 3.5 2.5 60 40 20 100 C 80 60 40 20 Particle Size (µm)

Figure 1: Particle size distribution of (a) FGD-C; (b) FGD-P; (c) FGD-I

Table 4: Particle size distribution of FGD wastes.

Parameter	FGD-C	FGD-P	FGD-I
D ₁₀ (μm)	6.273	2.877	5.340
$D_{50} (\mu m)$	36.734	21.138	23.747
D ₉₀ (µm)	191.812	89.955	78.206

3.3. Mineralogical composition

Figure 2-4 shows X-ray diffraction patterns (XRD) of the FGD samples, and the respective chemical compositions of crystalline phases are identified in Table 5-7.

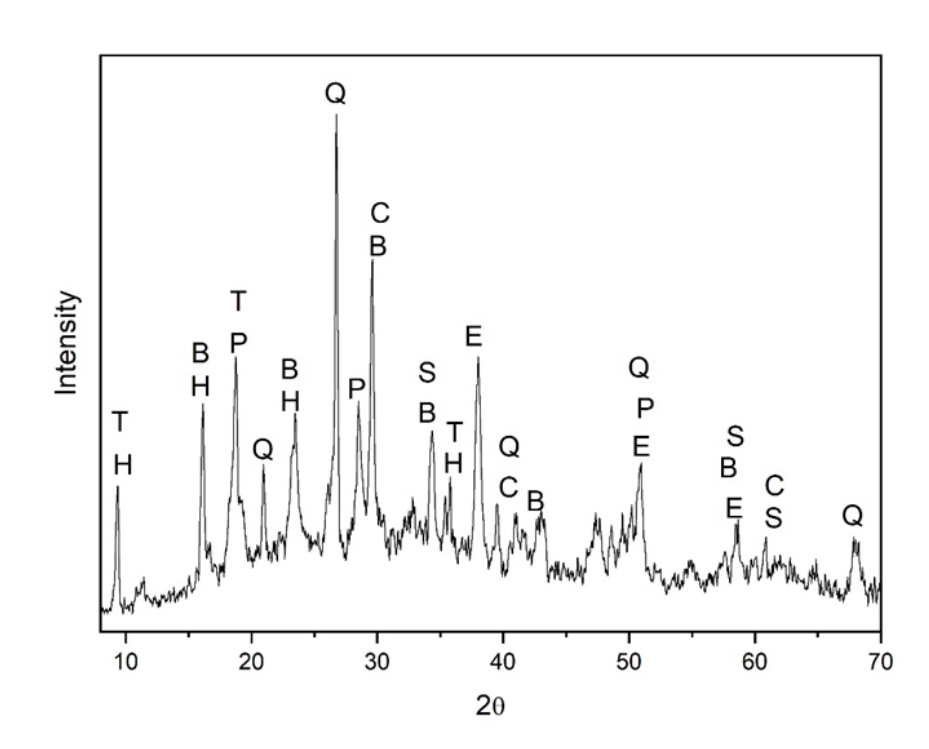
The FGD-C sample (Figure 2) presented an ettringite phase, which contains calcium and sulfate in its structure, and brucite phase, which are commonly found in residues from the process of wet desulfurization. Ettringite is formed due to hydration reactions that start between 10 and 50 days after application of water in the wet process. The presence of CaCO₃ indicates re-carbonation of Ca(OH)₂ by reaction with atmospheric CO₂. Based on the results, the FGD-C sample is a suitable alternative to replace natural gypsum.

X-ray diffraction analyses of FGD-I and FGD-P samples (Figure 3-4) revealed products that primarily contained CaSO₃.H₂O (hannebachite), formed in the desulfurization process by the semi-dry route. Portlandite present in all samples was derived from the use of excess sorbent [3].

The presence of quartz, the main component of fly ash, suggests that the reactions of calcium hydroxide with silica from the desulfurization process of the gas flux was not complete. The formation of crystalline aluminum compounds was only observed in the FGD-C sample of wet process.

Figure 2: XRD Pattern of FGD-C waste

(Q = Quartz, C = Calcite, T = Chabazite, P = Portlandite, S = Sodium carbonate, B = Brucite, E = Ettringite, H = Hydrated calcium aluminate hydroxide)



Compound	Formula
Quartz	SiO_2
Calcite	CaCO ₃
Chabazite	Ca _{1.979} Al _{3.8} Si _{8.2} O ₂₄
Portlandite	Ca(OH) ₂
Sodium carbonate	Na ₂ CO ₃
Brucite	$Mg(OH)_2$
Ettringite	Ca ₆ Al ₂ (SO ₄)(OH) ₁₂ .26 H ₂ O
Hydrated calcium aluminate hydroxide	Ca6Al2O6(OH)6.32 H2O

Table 5: Mineralogical composition of FGD-C waste.

Figure 3: XRD Pattern of FGD-P waste

 $(Q = Quartz, \ P = Portlandite, \ S = Sodium \ magnesium \ titanium \ oxide, \ H = Hannebachite,$ $C = calcium \ and \ iron \ oxide, \ L = Langbeinite \)$

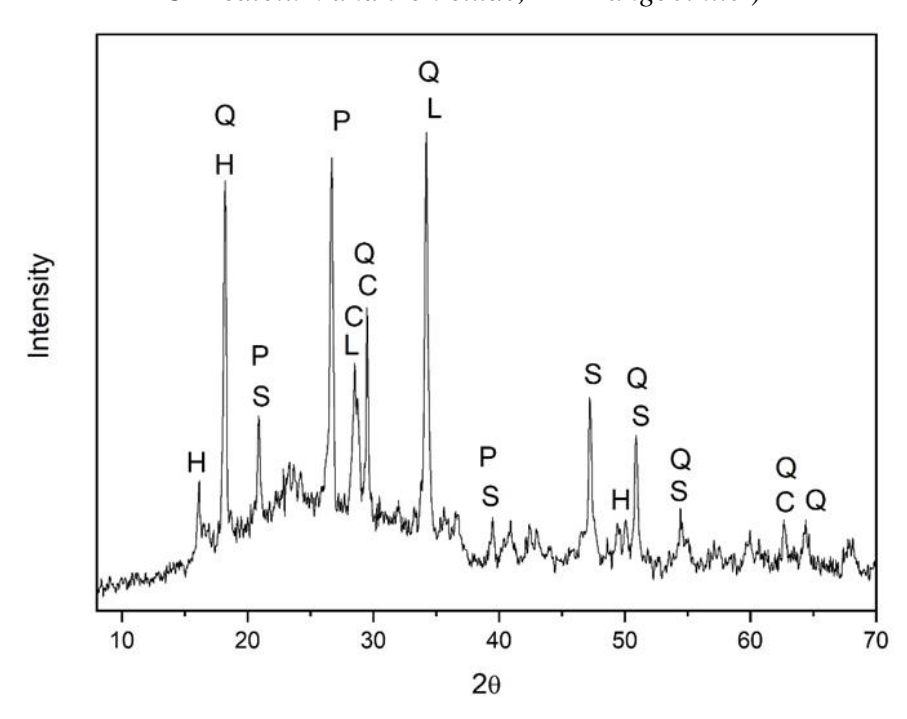


Table 6: Mineralogical composition of FGD-P waste.

Compound	Formula	
Quartz	SiO_2	
Portlandite	Ca(OH) ₂	
Sodium magnesium titanium oxide	$Na_{0.68}Mg_{0.34}Ti_{0.66}.O_2$	
Hannebachite	CaSO ₃ . H ₂ O	
Calcium and iron oxide	Ca ₂ Fe ₁₅ O ₂₅	
Langbeinite	$K_2Mg_2(SO_4)_3$	

Figure 4: *XRD Pattern of FGD-I waste*

(Q = Quartz, P = Portlandite, H = Hannebachite, C = calcium and iron oxide, L = Langbeinite)

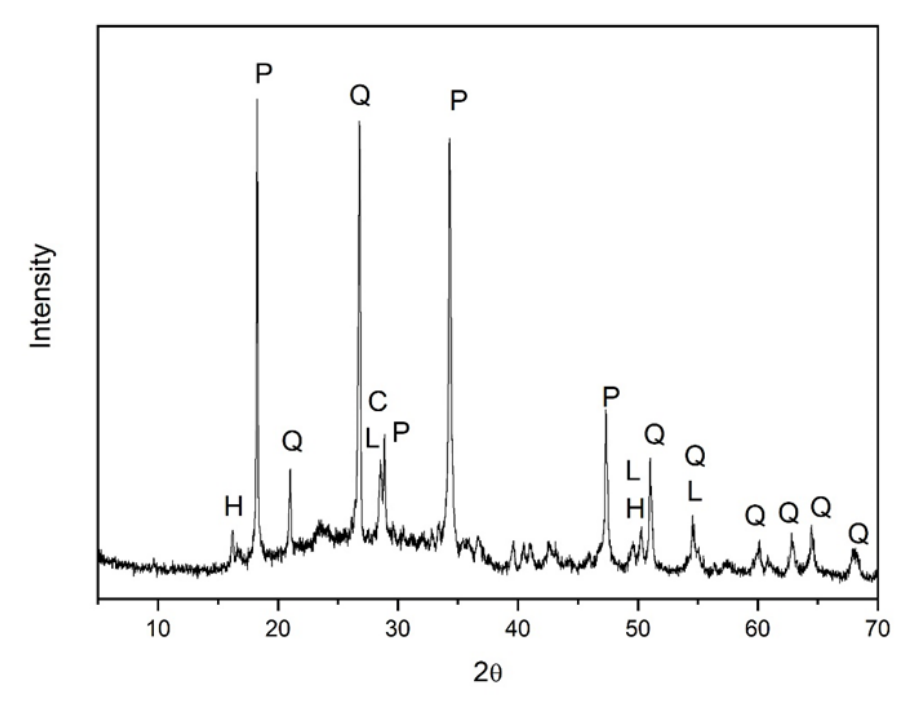


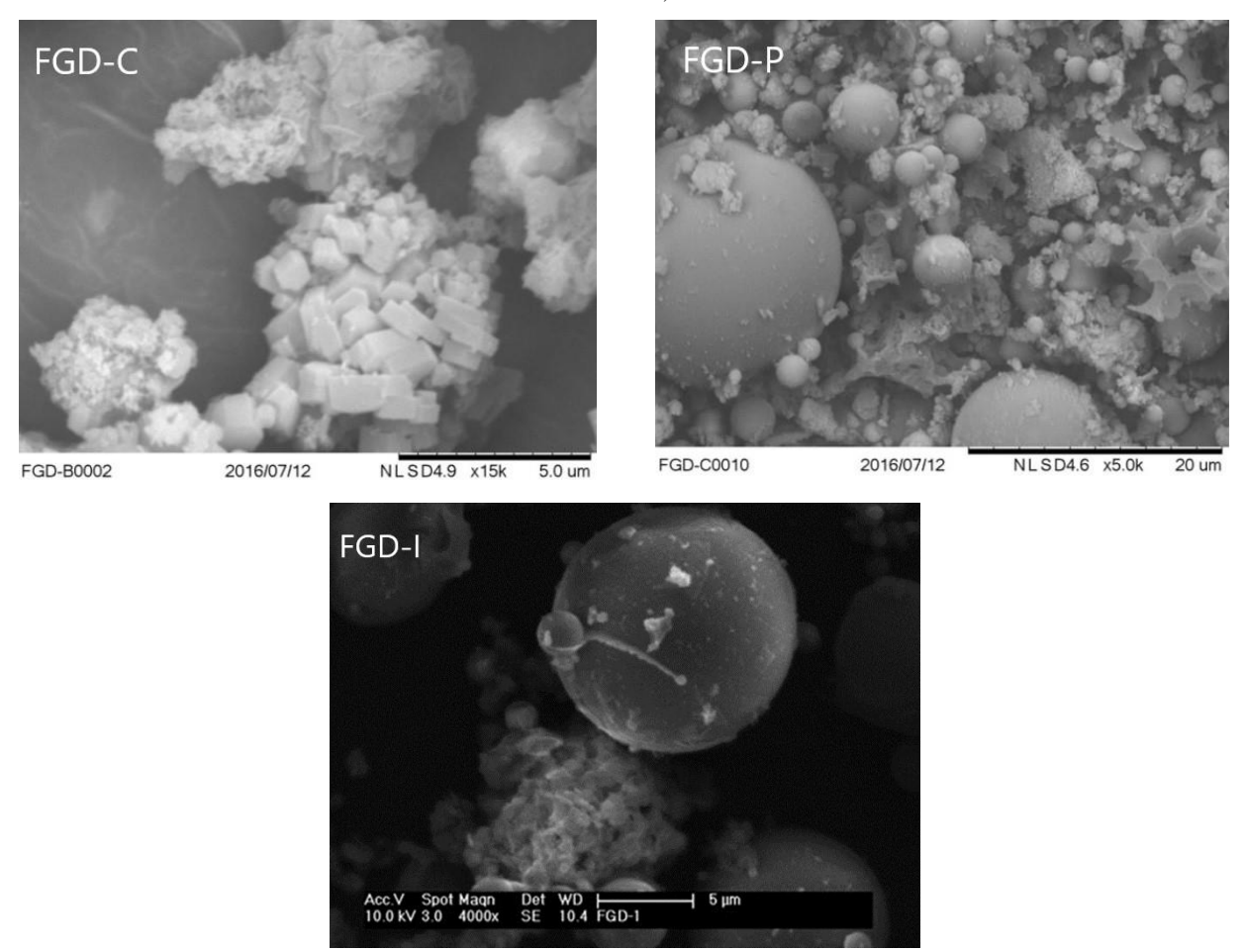
Table 7: Mineralogical composition of FGD-I waste

Compound	Formula
Quartz	${ m SiO_2}$
Portlandite	Ca(OH) ₂
Hannebachite	CaSO ₃ . H ₂ O
Calcium and iron oxide	$Ca_2Fe_{15}O_{25}$
Langbeinite	$K_2Mg_2(SO_4)_3$

3.4. Morphological characterization

The scanning electron micrographs of the FGD wastes are shown in Figure 5. The FGD samples presented heterogeneous particles with different diameters and shapes. Smooth surface spheres are usually silico-aluminous compounds, whereas irregular shapes particles with rough surface texture are unburnt coal, magnetic particles of iron oxide, amorphous particles which suffered a rapid cooling, or other types of minerals. In addition to the structures already mentioned, a large presence of rhombohedral crystals can be observed in FGD-C sample, also observed in other samples of FGD gypsum [23, 24].

Figure 5. SEM micrographs of wet FGD sample (FGD-C) and semi-dry FGD samples (FDG-P and FGD-I)



3.5. Leaching and solublization methods

FGD samples were submitted to leaching and solubilization tests for solid waste classification according to Brazilian regulation. The leaching and solublization tests were carried out in order to determine the potential leachability of selected elements, and the possibility of transferring those elements to the environmental media.

The leaching procedure is similar to the toxicity characteristic leaching procedure (TCLP) described in EPA method 1311. Solubilization test is applied to non-hazardous waste to establish it as inert or noninert, i.e., whether or not the parameters, after solubilization, are below maximum limits of potable water. According to these tests, the waste material can be classified as hazardous

(Class I) and as non-hazardous (Class II), being that Class II is divided into Class II A- not inert and Class II B- inert.

Table 8 and 9 shows the results of leaching and solubilization tests, respectively, and the maximum limit values determined by the Brazilian Standard Norm [25].

All element concentrations in the extract leachate of FGD samples (Table 8) were found to be below the maximum limit allowed (Annex F of the Norm ABNT NBR 10004), so the waste was considered Class II, non-hazardous waste.

Table 8: Concentration of elements leachate from FGD samples and the allowed limit values

Element	Leachate extract (mg L ⁻¹)			Allowed Limit (mg L ⁻¹)	
	FGD-I	FGD-P	FGD-P		
Ag	< 0.050	< 0.050	< 0.050	5.0	
As	0.238	0.179	0.193	1.0	
Ba	0.111	0.932	0.308	70	
Cd	0.014	0.013	0.014	0.5	
Cr	0.033	0.101	0.039	5.0	
Hg	< 0.006	< 0.006	< 0.006	0.1	
Pb	0.168	0.159	0.171	1.0	
Se	0.425	0.207	0.144	1.0	

Table 9 showed that concentrations of some elements of wet FGD and semi-dry FGD samples were above the maximum limit allowed (Annex G of the Norm ABNT NBR 10004). Therefore, according to solubilization results, the FGD samples can be classified as Class II A (non-inert) materials. The three combustion residues are non-hazardous solid waste that can be safely put into landfills.

Table 9: Concentration of elements solubilized from FGD samples and the allowed limit values

Element	Solubilized extract (mg L ⁻¹)			Allowed Limit	
				$(mg L^{-1})$	
	FGD-I	FGD-P	FGD-C		
Ag	< 0.050	< 0.050	< 0.050	0.05	
Al	0.141	0.112	0.095	0.2	
As	0.091	0.060	0.029	0.01	
Ba	0.120	6.39	0.072	0.7	
Cd	< 0.010	< 0.010	< 0.010	0.005	
Cr	0.475	0.191	0.018	0.05	
Cu	0.012	0.013	< 0.010	2.0	
Fe	0.052	< 0.050	< 0.050	0.3	
Hg	< 0.006	< 0.006	< 0.006	0.001	
Mn	0.051	< 0.010	< 0.010	0.1	
Na	57.0	136	70.8	200	
Pb	0.104	0.095	0.033	0.01	
Se	0.233	0.176	0.020	0.01	
Zn	0.028	< 0.010	< 0.010	5.0	

4. CONCLUSIONS

The natural radioactivity and trace elements concentrations in wet FGD and semi-dry FGD by-products arising from three different coal-fired power plants were evaluated. In general, the activity concentrations of 40 K is higher in FGD samples of semi-dry process. The activity concentrations of 238 U, 226 Ra, 232 Th and 40 K were lower than the worldwide average values for fly ash. The trace elements that showed the highest concentrations in decreasing order were Ba> Rb> Zr > Ce for all samples.

FGD samples were primarily composed of higher Ca, Si, S, Al and Fe content, and the main sulfur form is ettringite for wet FGD sample and hannebachite for semi-dry FGD samples. The particles of wastes presented rough surface texture, different crystal shapes and rhombohedral crystals in wet

FGD sample. Concentrations in the leachate and solubilized extract permits classifies the FGD samples as class II – not dangerous and class II A – not inert according to the Brazilian normative.

These results suggested that wet FGD can be used in production of eco-friendly cementitious matrices. Furthermore, due to its chemical composition, the three FGD samples can be used as raw material for the synthesis of value-added sorbents like zeolite and calcium silicate hydrate compound.

ACKNOWLEDGMENT

The authors are grateful to President Medici coal-fired power plant, Pecem coal-fired power plant and Itaqui coal-fired power plant for providing all samples for this study.

REFERENCES

- [1] CÓRDOBA, P. Status of Flue Gas Desulphurisation (FGD) systems from coal-fired power plants: Overview of the physic-chemical control processes of wet limestone FGDs. **Fuel**, v. 144, p. 274-286, 2015.
- [2] CASTRO, R. P. V; MEDEIROS, J. L.; ARAÚJO, O. Q. F.; CRUZ, M. A.; RIBEIRO, G. T.; OLIVEIRA, V. R. Fluidized bed treatment of residues of semi-dry flue gas desulfurization units of coal-fired power plants for conversion of sulfites to sulfates. Energy Convers Manag, v. 143, p. 173-187, 2017.
- [3] BIGHAM, J. M.; KOST, D. A.; STEHOUWER, R. C.; BEEGHLY, J. H.; FOWLER, R.; TRAINA, S. J.; WOLFE, W. E.; DICK, W. A. Mineralogical and engineering characteristics of dry flue gas desulfurization products. **Fuel**, v. 84, p. 1839-1848, 2005.
- [4] SHENG, G.H.; HUANG, P.; MOU, Y. Q.; ZHOU, C. H. Characteristics of fly ash from the dry flue gas desulfurization system for iron ore sintering plants. **Environ Technol**, v. 33, p. 837-844, 2012.
- [5] FUNGARO, D. A.; GROSCHE, L. C.; IZIDORO, J. C. Synthesis of Calcium Silicate Hydrate Compounds From Wet Flue Gas Desulfurization (FGD) Waste. J Appl Mater Technol, v. 1, p. 88–95, 2020.

- [6] GROSCHE, L. C.; BERTOLINI, T. C. R.; FUNGARO, D. A., Alkaline Hydrothermal Treatment of the Waste Produced in the Semi-Dry Flue Gas Desulfurization System. Int J Adv Res Chem Sci, v. 5, p. 9-19, 2018.
- [7] ROPER, A. R.; STABIN, M. G.; DELAPP, R. C.; KOSSON, D. S. Analysis of Naturally-occurring Radionuclides in Coal Combustion Fly Ash, Gypsum, and Scrubber Residue Samples. **Health Phys**, v.104, p. 264-269, 2013.
- [8] ROPER, A. R. Analysis of naturally occurring radionuclides in fly ash and gypsum samples. **Master of Science. Vanderbilt University**. 2012.
- [9] TAHA, R. Environmental and engineering properties of flue gas desulfurization gypsum. **Transp Res Rec**, p. 14-19, 1993.
- [10] ABNT NBR 10005 Brazilian Association of Technical Standards **Leaching Tests**, Rio de Janeiro, Brazil, p. 10, 2004.
- [11] ABNT NBR 10006 Brazilian Association of Technical Standards **Solubilization Tests**, Rio de Janeiro, Brazil, p. 2, 2004.
- [12] IAEA International Atomic Energy Agency. **Practical aspects of operating a neutron analysis laboratory. IAEA –TECDOC- 564**, Vienna: IAEA, 1999, 252p.
- [13] CUTSHALL, N. H.; LARSER, I. L.; OLSEN, C. R. Direct analysis of 210Pb in sediment samples: self-absorption corrections. **Nucl Instrum Methods Phys Res**, v. 206, p. 309-312, 1983.
- [14] UNSCEAR United Nations Scientific Committee on Effects of Atomic Radiation. Sources and effects of ionizing radiation. Exposures from Natural Radiation Sources, Annex B. New York: United Nations Publication, 2000.
- [15] KARDOS, R.; SAS, Z.; HEGEDUS, M.; SHAHROKHI, A.; SOMLAI, J.; KOVACS, T. Radionuclide content of NORM by-products originating from the coal-fired power plant in Oroszlány (Hungary). **Radiat Prot Dosim**, v. 167, p.266-269, 2015.
- [16] CÓRDOBA, S. P. Partitioning and speciation of trace elements at two coalfired power plants equipped with a wet limestone Flue Gas Desulphurisation (FGD) systems. **Thesis. Universitat Politècnica de Catalunya**. 2013.
- [17] CÓRDOBA, P. Partitioning and speciation of selenium in wet limestone flue gas desulphurisation systems: A review. **Fuel**, v. 202, p. 184-195, 2017.

- [18] FGD HANDLING Review of handling and use of FGD material. **CARRC Topical Report. U.S. Department of Energy**. 2003. 43p.
- [19] KOST, D. A; BIGHAM, J. M.; STEHOUWER, R.C.; BEEGHLY, J.H.; FOWLER, R.; TRAINA, S. J.; WOLFE, W. E.; DICK, W. A. Chemical and physical properties of dry flue gas desulfurization products. **J Environ Qual**, v. 34 p. 676-686, 2005.
- [20] EPRI A Review of Literature Related to the Use of Spray Dryer Absorber Material: Production, Characterization, Utilization Applications, Barriers, and Recommendations. Technical Report, ND: 1014915. 2007, 108 p.
- [21] DEPOI, F. S.; POZEBON, D.; KALKREUTH, W. D. Chemical characterization of feed coals and combustion-by-products from Brazilian power plants. **Int J Coal Geol**, v. 76, p. 227-236, 2008.
- [22] HANSEN, B. B.; KIIL, S., Investigation of Parameters Affecting Gypsum Dewatering Properties in a Wet Flue Gas Desulphurization Pilot Plant. **Ind Eng Chem Res**, v. 51, p. 10100-10107, 2012.
- [23] BAKSHI, P.; PAPPU, A; GUPTA, M. K. Flue Gas Desulphurization (FGD) Gypsum Waste -Recycling Opportunity. In: **Annual Technical Volume on "Technologies for Zero Waste in India: Current and Future Challenges"**, Environmental Engineering Division Board, ISBN: 978-81-952159-4-2, 2021, p. 68-73.
- [24] WANG, X.; WANG, L.; WANG, Y.; TAN, R.; KE, X.; ZHOU, X.; GENG, J.; HOU, H.; ZHOU, M. Calcium Sulfate Hemihydrate Whiskers Obtained from Flue Gas Desulfurization Gypsum and Used for the Adsorption Removal of Lead. **Crystals**, v. 7, p. 270-290, 2017.
- [25] ABNT BR 10004 Brazilian Association of Technical Standards **Solid Waste - Classification**, Rio de Janeiro, Brazil, p. 16, 2004.

This article is licensed under a Creative Commons Attribution 4.0 International License, which permits use, sharing, adaptation, distribution and reproduction in any medium or format, as long as you give appropriate credit to the original author(s) and the source, provide a link to the Creative Commons license, and indicate if changes were made. The images or other third-party material in this article are included in the article's Creative Commons license, unless indicated otherwise in a credit line to the material.

To view a copy of this license, visit http://creativecommons.org/ licenses/by/4.0/